ECCOMAS Congress 2016
VII European Congress on Computational Methods in Applied Sciences and Engineering
M. Papadrakakis, V. Papadopoulos, G. Stefanou, V. Plevris (eds.)
Crete Island, Greece, 5–10 June 2016

SIMPLE CLOSED FORM HOMOGENIZATION MODEL FOR THE NON LINEAR STATIC AND DYNAMIC ANALYSIS OF RUNNING BOND MASONRY WALLS IN AND OUT OF PLANE LOADED

Elisa Bertolesi, Gabriele Milani*

Department ABC
Technical University of Milan
Piazza Leonardo da Vinci 32, Milan, Italy
{gabriele.milani,elisa.bertolesi}@polimi.

Keywords: masonry; holonomic model; closed form solution; non-linear static analysis; non-linear dynamic analysis.

Abstract. *A simple total displacement homogenization model suitable for the non-linear analysis of in and out of plane loaded masonry walls is presented. In the model, a running bond rectangular elementary cell is discretized into few triangular elastic constant stress elements representing bricks and non-linear holonomic with softening mortar joints reduced to interfaces. The unrefined discretization adopted allows dealing with a homogenization problem ruled by few displacement variables, where homogenized stress-strain relationships can be found in semi-analytical form.*

The approach proposed is validated at a cell level in both the elastic and inelastic range, exhibiting excellent numerical stability and accuracy.

It finally allows a straightforward implementation at a structural level on a commercial code, where entire walls are modelled by means of rigid elements and non-linear homogenized interfaces. Some example of technical relevance are analyzed in both the non-linear static and dynamic range and compared with those achieved using alternative numerical procedures. To this aim a first set of simulation is performed on a deep beam tested by Page while the second series of analyses are conducted on a church façade subjected to dynamic excitation.

1 INTRODUCTION

Masonry is a traditional composite material obtained by the assemblage of bricks and mortar. The elastic behavior is quite limited because masonry is typically characterized by a reduced, almost vanishing tensile strength and either macro- or micro-modeling strategies are adopted over elasticity.

Macro-modeling [1]-[3] substitutes bricks and mortar with a homogeneous, sometimes orthotropic material with softening. It allows studying even large scale structures without the need of meshing separately bricks and mortar. It is therefore very convenient where efficient computations on engineering structures are needed. Nevertheless, the calibration of model parameters is typically done by means of comprehensive experimental campaigns. Theoretically, such approaches may be capable of adequately estimate the non-linear masonry behavior along any load combination, even if some meaningful limitations occur in specific cases but in practice the needed experimental data fitting would require –at least in principle- new calibrations case by case.

The alternative micro-modeling is simply characterized by a distinct modelling of mortar joints and blocks at a structural level. The reduction of joints to interfaces [4][5] helps in limiting variables, especially in the non-linear range, but the approach still remains computationally very demanding, because bricks and mortar are meshed separately. In order to obtain sufficiently reliable solutions in terms of displacements and stresses, constituent materials should be meshed with more than one element, with the consequent grow of the number of non-linear equations to deal with, even for small masonry panels. Furthermore, the preprocessing phase regarding the model generation is not straightforward. Partitioning methods have been recently proposed to overcome such computational limitations and speed up structural analyses.

For the previous reasons, it can be affirmed that macro-scale computations with FEs still remain preferable when non-linear analyses for engineering structures are needed.

In this framework, homogenization [5]-[16] is for sure much more suitable than both micro- and macro-modelling, because it allows in principle to perform non-linear analyses of engineering interest without a distinct representation of bricks and mortar, but still considering their mechanical properties and the actual pattern at a cell level.

Homogenization is roughly an averaging procedure performed at a meso-scale on a representative element of volume (REV), which generates the masonry pattern under consideration by repetition. A Boundary Value Problem BVP is formulated, allowing an estimation of the expected average masonry behavior to be used at structural level. As a matter of fact, the resultant material obtained from meso-scale homogenization turns out to be orthotropic, with softening in both tension and compression.

Instead of using refined FE discretization within the REV, in this paper a simplified homogenization two-step model is proposed for the non-linear structural analysis of masonry walls in- and out-of-plane loaded. The first step is applied at the meso-scale, where the assemblage of bricks and mortar in the REV is substituted with a macroscopic equivalent material through a so called compatible identification. The unit cell is meshed by means of 24 triangular constant stress (CST) plane stress elements (bricks) and interfaces for mortar joints. Triangular elements are assumed linear elastic, whereas the mechanical response of the interface elements is holonomic and non-linear, including two dominant deformation modes, namely peel (mode I) and shear (mode II) or a combination of two (mixed mode). Both a piecewise linear and an exponential law formally identical to an improved version of the Xu-Needleman law and proposed in another context [17]-[19] are implemented.

The second step, performed at a structural level, relies into the implementation of the homogenized stress-strain relationships into a rigid element approach (RBSM) where contiguous rigid elements are connected by shear and normal non-linear homogenized springs. The extension of the model to the out-of-plane mechanisms has been achieved by on-thickness integration of the homogenized stress-strain relationships obtained in the first step, thus adopting suitable out-of-plane interface laws at a structural level, whose behavior is formulated in order to describe flexural and torsional failures.

The procedure is quite efficient and reliable because it is not necessary to discretize with refined meshes the elementary cell (only three kinematic variables are needed at the meso-scale) and hence it is possible to drastically speed up computations. In addition, the holonomic laws assumed for mortar allow for a total displacement formulation of the model, where the only variables entering into the homogenization problem are represented by displacements.

The model is benchmarked at a structural level both in the non-linear static and dynamic range on a masonry deep-beam [20][21] in-plane loaded up to collapse and on a masonry church façade [22][23] loaded by a real accelerogram and collapsed during the 1976 Friuli (Italy) seismic sequence [24].

2 THE HOMOGENIZATION MODEL

2.1 The simplified compatible homogenization model

Homogenization relies in the determination of averaged quantities representing the macroscopic strain and stress tensors [1][6] on a REV (Y), i.e. $\mathbf{E} = <\boldsymbol{\varepsilon}> = \frac{1}{A}\int_Y \boldsymbol{\varepsilon}(\mathbf{u})dY$ and $\boldsymbol{\Sigma} = <\boldsymbol{\sigma}> = \frac{1}{A}\int_Y \boldsymbol{\sigma} dY$, where A stands for the area of the elementary cell, $\boldsymbol{\varepsilon}$ and $\boldsymbol{\sigma}$ stand for the local quantities (strains and stresses respectively) and <*> is the averaging operator.

Anti-periodicity conditions are imposed on the stress field and periodicity on the displacement field **u**, given by:

$$\begin{cases} \mathbf{u} = \mathbf{E}\mathbf{y} + \mathbf{u}^{\text{per}} \quad \mathbf{u}^{\text{per}} \text{ on } \partial Y \\ \boldsymbol{\sigma}\mathbf{n} \quad \text{anti-periodic} \quad \text{on } \partial Y \end{cases} \tag{1}$$

Where **u** is the total displacement field, $\mathbf{u}^{\text{per}}$ stands for a periodic displacement field, $\widetilde{x} = \{x \quad y \quad z\}$ is the local frame of reference (see Figure 2), **E** is the homogenized strain tensor and **n** is the outward versor of the ∂Y surface.

In this work, a simple compatible homogenization model suitable for the analyses of masonry in and out of plane loaded is proposed. The method herein discussed allows to use a coarse discretization, where only ¼ of the REV is meshed with 6 constant stress triangles (see Figure 1). Bricks are supposed to behave elastically while mortar joints are reduced to non-linear zero thickness interfaces. Two interface relationships are considered: a piece-wise linear law and an improved version of the Xu-Needleman exponential law, accounting for, respectively, a decoupled and fully coupled approach.

The homogenization procedure is subdivided in two steps: in the first one the homogenization model is implemented in a Matlab environment, while in the second one a series of non-linear analyses on masonry panels are discussed.

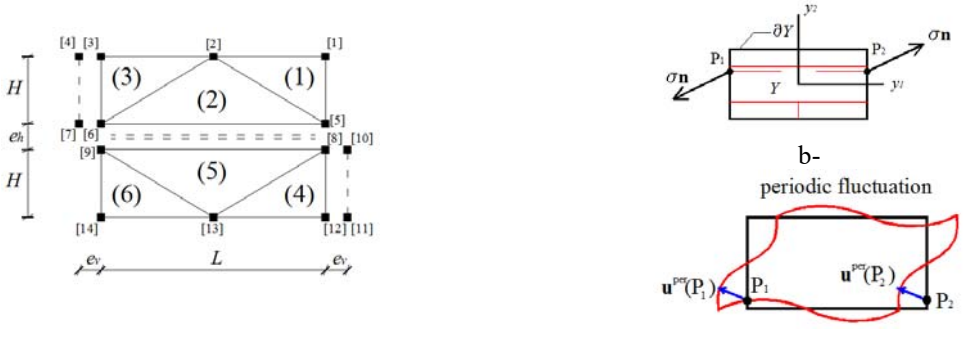

Figure 1. Micro-mechanical model proposed: a- Geometric properties of the elementary cell, b- Anti-periodicity of the micro-stress field and c- periodic displacement field.

Indicating with $\circ^{(n)}$ a stress component belonging to the n-th element, the plane stress Cauchy stress tensor inside the n-th CST element $\boldsymbol{\sigma}^{(n)}$ is constituted by the components $\sigma_{xx}^{(n)}$ (horizontal stress), $\sigma_{yy}^{(n)}$ (vertical stress) and $\tau^{(n)}$ (shear stress). When dealing with static quantities, equilibrium inside each element is a-priori satisfied, $div\boldsymbol{\sigma}=0$, whereas two equality constraints involving Cauchy stress tensor components of triangles have to be imposed for each internal interface between adjoining elements.
Assuming that the triangular elements are linear elastic, the following relationship between strains and stresses can be written:

$$\begin{bmatrix}\varepsilon_{xx}\\ \varepsilon_{yy}\\ \gamma_{xy}\end{bmatrix}=\begin{bmatrix}\dfrac{\sigma_{xx}}{E_b}-\dfrac{\nu_b\sigma_{yy}}{E_b}\\ -\dfrac{\nu_b\sigma_{xx}}{E_b}+\dfrac{\sigma_{yy}}{E_b}\\ \dfrac{\tau}{G_b}\end{bmatrix} \qquad (2)$$

Where E_b, ν_b and G_b are the brick elastic modulus, Poisson's ratio and shear modulus, respectively. The simplified compatible identification procedure allows separating the analyses of the biaxial macroscopic strain state from the pure shear deformation one. In the following sections both deformation states are discussed and the results obtained using both the non-linear interface laws are critically compared.

2.2 Elastic case, biaxial strain state

Let us consider a biaxial macroscopic strain state characterized by the following independent displacement variables: $\xi=\bar{U}_x^0-U_x^9$ and $\eta=U_y^{[5]}+U_y^{[6]}$. The evaluation of the aforementioned variables allows the determination of the kinematic and static unknowns governing the problem. The solution, fully explained in [9], can be obtained graphically plotting the two following curves:

$$\eta=\bar{U}_y^0+\frac{2H}{\nu_b L}\left[\bar{U}_x^0-\xi-L\frac{1-\nu_b^2}{E_b}f_n^I(\xi)-\frac{L^2}{2H}\frac{1-\nu_b^2}{E_b}f_t^{II}(\xi)\right] \qquad (3)$$

$$\xi = \bar{U}_x^0 + \frac{L}{2\nu_b H}\left[\bar{U}_y^0 - \eta - 2\frac{1-\nu_b^2}{E_b} H f_n^{II}(\eta)\right] \tag{4}$$

Where f_n^I and f_t^{II} are the non-linear laws of the interfaces I and II under normal (n) and shear (t) stresses. $\overline{U}_{x,y}^0$ are the applied displacements on the boundary of the REV mimicking a macroscopic homogeneous biaxial strain state, in agreement with the compatible identification procedure proposed.

2.3 Shear deformation

In case of a pure shear deformation, the deformation independent variables are ξ^t, η^t and κ, where:

$$\xi^t = 2\bar{U}_x^t - \frac{H}{G_b}\left[-\frac{\bar{U}_y^t - \eta^t}{L/2} G_b + 2 f_t^I\left(\eta^t\right) - \frac{4H}{L} f_n^{II}\left(\eta^t - \kappa\right) + 2\frac{\kappa}{L} G_b\right] \tag{5}$$

$$\eta^t = \bar{U}_y^t - \frac{L}{2G_b}\left[2 f_t^{II}\left(\xi^t - \bar{U}_x^t\right) - \frac{2\bar{U}_x^t - \xi^t}{H} G_b + 2\frac{\kappa}{L} G_b\right] \tag{6}$$

$$\kappa = \frac{e_V}{G_b}\left[2 f_t^{II}\left(\xi^t - \bar{U}_x^t\right) - f_t^I\left(\eta^t\right)\right] \tag{7}$$

$\overline{U}_{x,y}^t$ are the applied displacements on the boundary of the REV mimicking a macroscopic shear, in agreement with the compatible identification procedure proposed. The numerical approach used to solve the previous problem is discussed in [9], where the reader is referred for further details.

2.4 Holonomic relationship for non-linear interfaces

In the present work, mortar joint interfaces are assumed to behave in agreement with two interface relationships: (a) a multi-linear relationship, hereafter labeled as "PL", with normal and tangential decoupled responses, i.e. $\sigma(\Delta_n)$ and $\tau(\Delta_t)$; an improved version of the Xu–Needleman exponential law, hereafter labeled as "XN". In the latter case, the stress vector **T** at the interface is given by the following closed-form expression:

$$\begin{aligned}
\sigma &= \frac{\phi_n}{\delta_n}\left(\frac{\Delta_n}{\delta_n}\right) e^{-\left(\frac{\Delta_t}{\delta_t}\right)^2} e^{-\frac{\Delta_n}{\delta_n}} \\
\tau &= 2\frac{\phi_t}{\delta_t}\left(\frac{\Delta_t}{\delta_t}\right)\left(1 + \frac{\Delta_n}{\delta_n}\right) e^{-\left(\frac{\Delta_t}{\delta_t}\right)^2} e^{-\frac{\Delta_n}{\delta_n}}
\end{aligned} \tag{8}$$

Symbols ϕ_n and ϕ_t denote the work of separation under pure Mode I and Mode II, respectively, while δ_n and δ_t indicate the relevant characteristic lengths [17][19].

2.5 Non-linear behavior

In the present section the results obtained with the proposed model are discussed with reference to two masonry patterns commonly used.
Two different textures are studied: the first one (Type A) is a running bond masonry with bricks having dimensions equal to 122x37x54 mm^3 and mortar joints of thickness 5 mm (see

Figure 2). The second one (Type B) is a header bond with blocks of dimensions 250x55x120 mm^3 and mortar joints 10 mm thick.

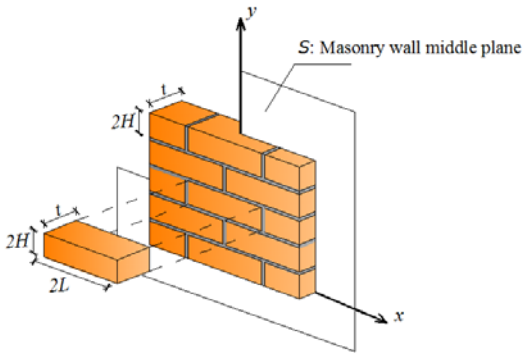

Figure 2. Running bond texture.

The elastic and inelastic mechanical properties of the considered masonry patterns are summarized in Table 1-Table 2.

Table 1. Mechanical properties assumed for the running bond texture.

Stretcher bond	*Mortar joints*	*Bricks*
Young Modulus	E_m=1250 MPa	E_m=7000 MPa
Poisson's ratio	-	ν=0.2
Shear Modulus	G_m=0.4* E MPa	G_b
Peak tensile stress	f_t= 0.29 MPa	-
Cohesion	c=1.4* f_t MPa	-

Table 2. Mechanical properties assumed for the running bond texture.

Stretcher bond	*Mortar joints*	*Bricks*
Young Modulus	E_m=1500 MPa	E_m=8000 MPa
Poisson's ratio	-	ν=0.2
Shear Modulus	G_m=0.4* E MPa	G_b
Peak tensile stress	f_t= 0.1 MPa	-
Cohesion	c= 0.1 MPa	-

Both a PL and XN holonomic law (for the sake of brevity only Type A masonry interfaces are depicted in Figure 3) has been adopted for mortar joints.

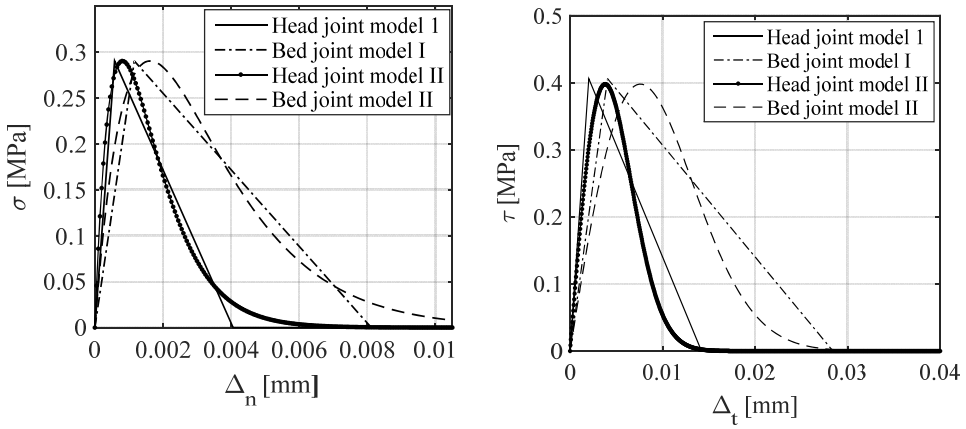

a- b-

Figure 3. Running bond model (Type A): Normal (a-) and tangential (b-) behavior.

3 INELASTIC CASE, BIAXIAL AND SHEAR DEFORMATIONS

3.1 Biaxial strain state

The homogenization approach discussed in the previous sections is herein adopted to perform a series of analyses at a cell level taking into account the non-linear behaviour of the mortar joint interfaces. Let us consider the strain E_{nn} defined as $E_{nn} = \sqrt{E_{xx}^2 + E_{yy}^2}$. In Figure 4, the homogenized stress-strain relationship obtained using the proposed model and assuming an $E_{xx} \neq 0$ and $E_{yy} = 0$ strain state applied up to failure of the REV is depicted. In Figure 4 the deformed shapes of the elementary cell at three different steps of the analysis (A elastic, B peak and C failure) are also represented (Type A and Type B).

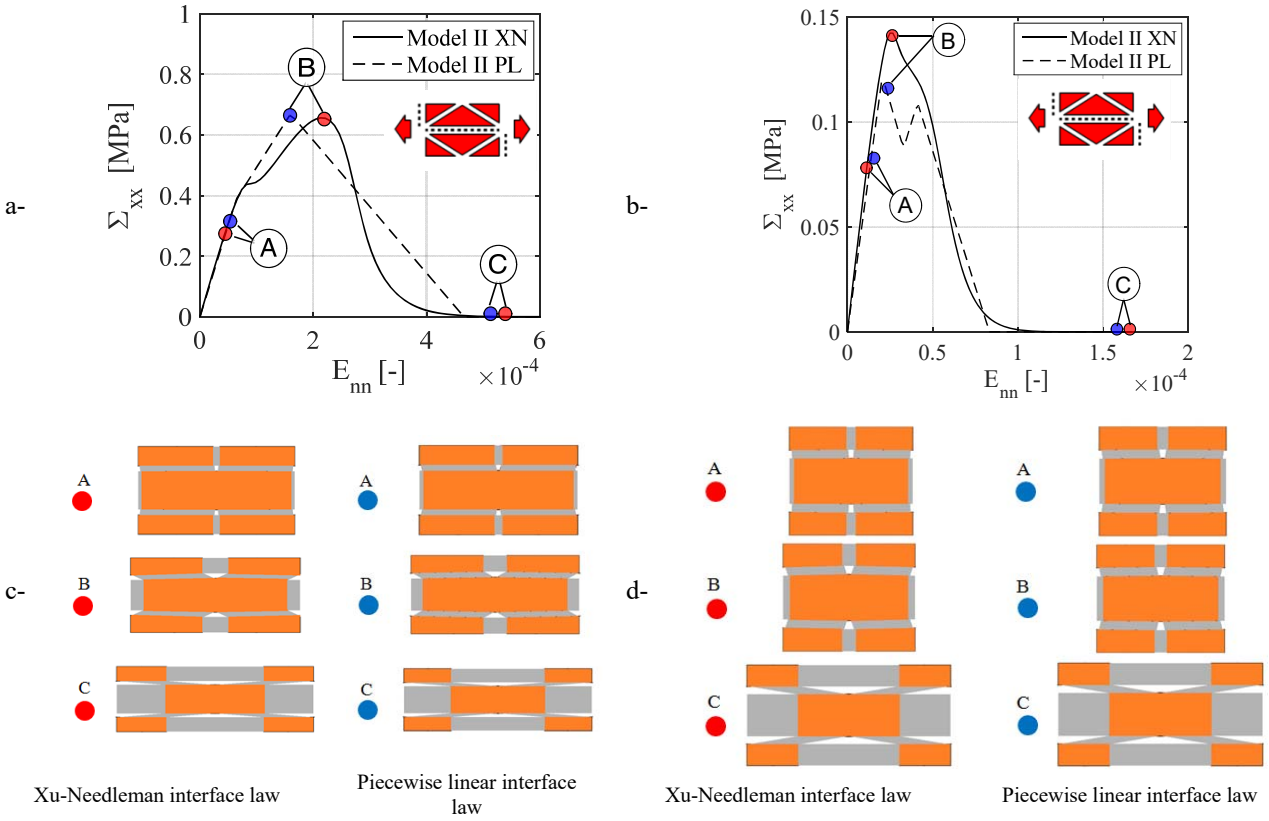

Figure 4. Homogenized stress-strain curves (Type A texture) (a-) and (Type B texture) (b-), deformed shapes of the homogenized cell at different steps for horizontal stretching, Type A texture c- and Type B texture d-.

The same results in case of application of $E_{yy} \neq 0$ and $E_{xx} = 0$ are summarized in Figure 5 (Type A) and (Type B). The reader is referred to [16] for further details.

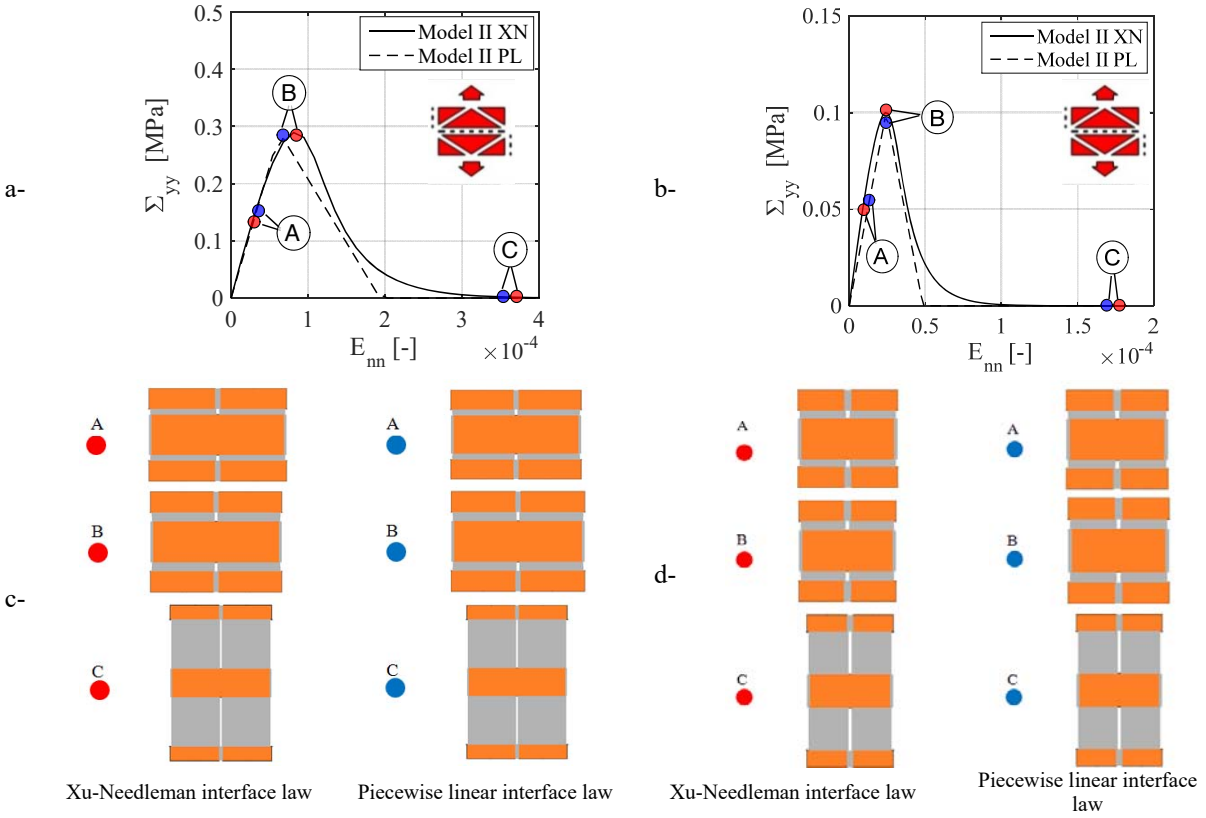

Figure 5. Homogenized stress-strain curves (Type A texture) (a-) and (Type B texture) (b-), deformed shapes of the homogenized cell at different steps for vertical stretching, Type A texture c- and Type B texture d-.

From an analysis of the results, the following considerations can be done:
- When dealing with a biaxial strain state both interface models furnish comparable outputs. Some differences can be found due to the coupling between normal and transversal response in the XN law.
- Under horizontal stretching (see Figure 4), a not-negligible shear stress is detected. The failure mechanism of the REV is characterized by bed joint cracking under tangential stresses while head joints fail under normal tensile stresses.
-For vertical stretching (see Figure 5) the failure experienced is always on the bed joint and strongly influenced by the value of the ultimate tensile strength adopted for mortar.

3.2 Shear deformation state

The results obtained applying a pure shear deformation state on the elementary cell are depicted in Figure 6 for Type A and Type B masonries. As expected in both cases both head and bed joint exhibit inelastic deformation that contributes to the overall strength and post peak behavior of the elementary cell.

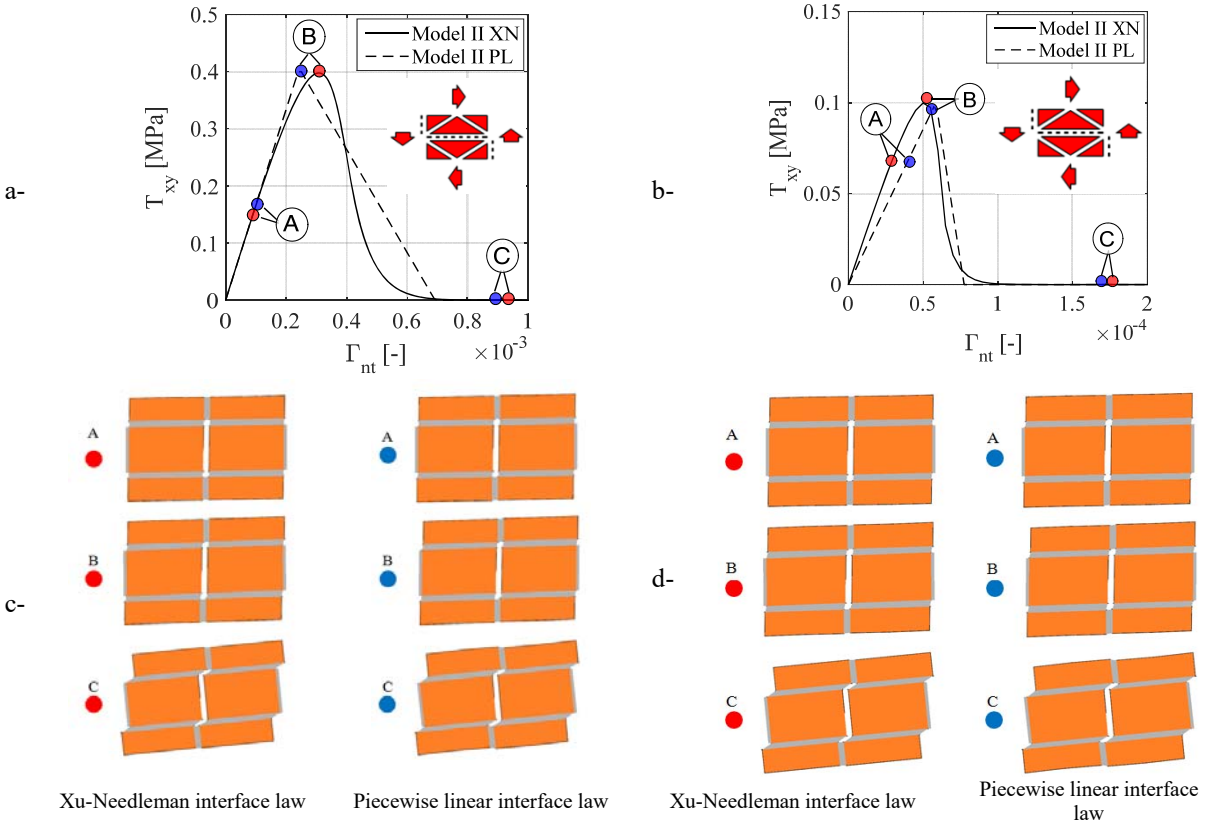

Figure 6. Shear deformation state (Type A texture) (a- c-) and (Type B texture) (b- d-).

4 STRUCTURAL IMPLEMENTATION

4.1 Rigid body and spring model

The present section is devoted to the discussion of a series of non-linear analyses performed in order to show the capability of the proposed model for the simulation of large scale panels subjected to different load conditions. All the analyses performed are conducted through the commercial software Abaqus, were the homogenized mechanical properties are implemented. The panels simulated are discretized by means of rigid quadrilateral elements connected with non-linear interfaces exhibiting an orthotropic behaviour. The interfaces are assumed to obey stress-strain curves with softening directly deduced by an energy equivalence criterion with the homogenized material. The method adopted for the spring identification will be briefly recalled in the following, but the reader is referred to [16] for further details.
In order to perform the identification of the springs two adjoining rigid elements connected through non-linear interfaces with dimensions showed in Figure 7 were considered.

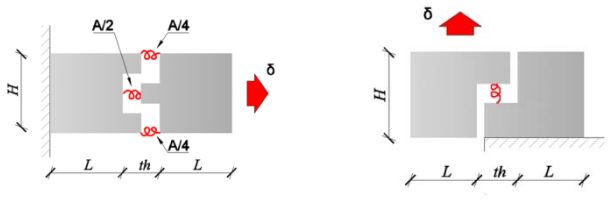

a- b-

Figure 7. Spring model: a- Axial spring, b- Shear spring.

Equating the volumetric strain energy of the rigid-spring model and the one related with the continuum, the following expressions can be deduced for the identified elastic moduli:

$$E_{nxx} = \frac{th/2 \cdot E_{xx}}{2L + th} \tag{8}$$

$$E_{nyy} = \frac{th/2 \cdot E_{yy}}{H + th} \tag{9}$$

$$G_{nxy} = G_{xy} \cdot \frac{H^2/4}{th \cdot (2L + th)} \tag{10}$$

Where H and L are respectively the height and the length of the rigid elements and "t" is the out of plane thickness. The non-linear interfaces have thickness equal to "th". E_{xx}, E_{yy} and G_{xy} are the elastic properties of the homogenized orthotropic continuum model.
The procedure previously recalled is adopted even for the definition of the elastic properties of out of plane interfaces. The extension of the model to the out-of-plane mechanisms has been achieved adopting suitable interfaces, whose behaviors have been formulated in order to describe flexural and torsional failures. To this aim the following expressions can be obtained. Where "t" refers to the thickness of the rigid quadrilateral elements, while "E_{bxx}", "E_{byy}" and "G_{bxy}" refer respectively to the elastic properties of the flexural and torsional interfaces.

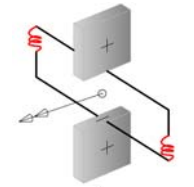

$$E_{bxx} = \frac{E_{xx}}{(1-\upsilon^2)} \cdot \frac{t \cdot th \cdot L}{12 \cdot 2 \cdot A_b \cdot (H + th)} \tag{11}$$

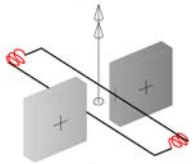

$$E_{byy} = \frac{E_{yy}}{(1-\upsilon^2)} \cdot \frac{t \cdot th \cdot L}{12 \cdot 2 \cdot A_b \cdot (H + th)} \tag{12}$$

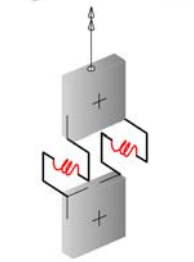

$$G_{bxy} = \frac{2G_{xy} \cdot t^4}{3th \cdot L^3} \tag{13}$$

4.2 Deep beam test

The previously discussed procedure is used to simulate a deep beam panel tested up to failure by Page [20]. The wall, with dimensions of 757x457 mm^2, was subjected to a uniform pressure applied by a stiff steel beam placed on the central upper part of the panel.
A running bond texture (Type A) was adopted to build the panel, using half scale bricks with dimensions equal to 122x37x54 mm^3 and 5 mm thick mortar joints.
The springs identification discussed in the previous section, led to use the following moduli for the springs: E_{nxx}= 360 MPa, E_{nyy}= 280 MPa and G_{nxy}= 2840 MPa.

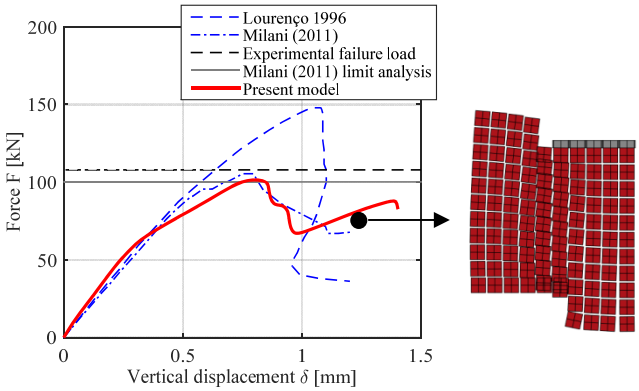

Figure 8. Deep beam. Numerical and experimental results.

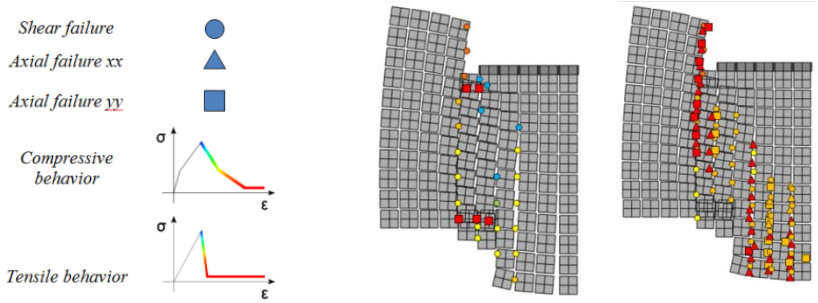

a- b-

Figure 9. Deep beam. Damage maps in compression (-a) and in tension (-b).

Despite the exiguous number of information reported by Page, in the recent past several researchers have tried to simulate the aforementioned deep beam test using different numerical approaches. A comparison between the results (force displacement curves) obtained using the present model and those found numerically by Lourenço [21] and Milani [13] is shown in Figure 8.

As can be noted, a satisfactory agreement is found, in terms of both elastic and post peak phase. The collapse load obtained numerically is very close to the value found experimentally by Page. In Figure 9 the damage maps obtained numerically at the end of the simulation are shown, in compression, tension and shear.

As can be noted, the collapse mechanism is clearly formed by a compressive strut departing from the steel beam and ending on the support, with shear cracks appearing on a vertical line (orange circles, Figure 9-a) and compressive damages near the toe (red squares, Figure 9-a). Tensile damages are mainly concentrated in the central part of the panel along vertical interfaces and near the steel beam. This latter finding can be explained with the high level of stress concentrations reached in that zone.

4.3 Transfiguration church non-linear static and dynamic analyses

A second series of simulations is performed with reference to 3D masonry structures subjected to both static and dynamic excitations, under in- and out-of-plane loads. As confirmed in the literature, some classes of buildings are particularly prone to experience severe damages during seismic events, among them masonry churches can be mentioned. In order to show how accurate results can be obtained using the proposed model even in presence of out of plane failure mechanisms, the authors chose to analyze the façade of the Transfiguration Church, collapsed during the 1976 Friuli, Italy seismic sequence. The church under considera-

tion was located in Moggio Udinese, in the North-East of Italy, in a region (called Friuli) characterized by a high seismicity level. On Thursday, 6 May 1976, a devastating 6.4 Richter magnitude earthquake took place there, killing 989 people. The church reported severe damage after the first main shock, and later collapsed as a consequence of the second seismic sequence that occurred during September of the same year. After the first main earthquake, a survey of the geometry and masonry walls was conducted by Doglioni et al. in [24], which is our main source of information for the problem at hand. The geometry of the façade, along with the discretization adopted for the present structural analyses are sketched in Figure 10. It is interesting to notice that a small portion of the unique nave perpendicular walls is modeled in order (a) to properly account for the actual lateral interlocking of the vertical edges and (b) to favor the reproduction of the 3D behavior, which includes a predominant two-way flexural deformation and a possible detachment for overturning in case of insufficient interlocking between façade and nave walls.
The façade of the Church is modeled using 354 rigid quadrilateral elements, which appears a fair compromise between numerical efficiency paramount for non-linear dynamic computations and refinement needed to properly reproduce actual crack patterns.
The church can be considered an example of Romanesque architecture quite frequent in the small towns of Italy, like those located in Friuli, and therefore it appears an interesting benchmark for the proposed models at the macro-scale. Approximately, the façade has a width of 16.30 meters, with a maximum height (tympanum top) of 18.05 meters and small openings in correspondence of the symmetry axis, see Figure 10. The façade has therefore global dimensions equal to 16.30x18.05 m, with walls 55 cm thick. Mechanical properties of the constituent materials are assumed in agreement with those available in the literature [22][23] and are not reported here for the sake of conciseness. Homogenized moment-curvature diagrams obtained with the model proposed and used at a structural level are depicted in Figure 11, under three levels of vertical pre-compression roughly indicating what occurs on the tympanum (almost zero vertical in-plane load), middle height and base of the façade. The utilization of different moment-curvature relationships as a function of vertical membrane load is paramount for masonry buildings, since it has been proved that vertical compression plays a key role in the increase of both ductility and out-of-plane strength.

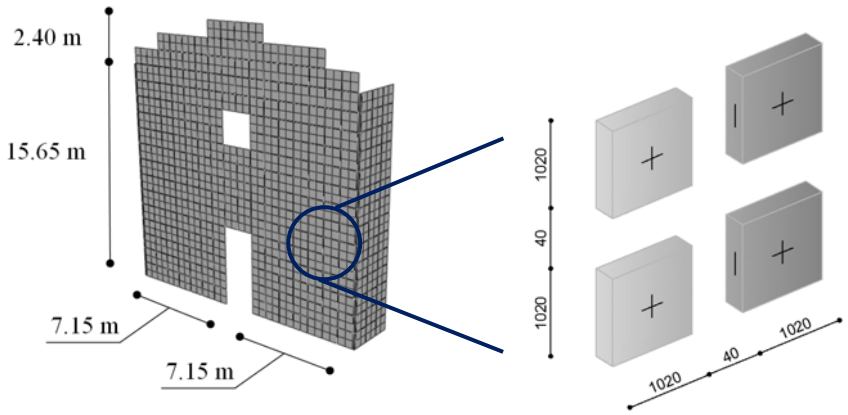

-a -b

Figure 10. Non-linear static and dynamic analysis of a church façade in Moggio Udinese (Transfiguration Church). –a: Geometric description of the case study. –b: FE discretization.

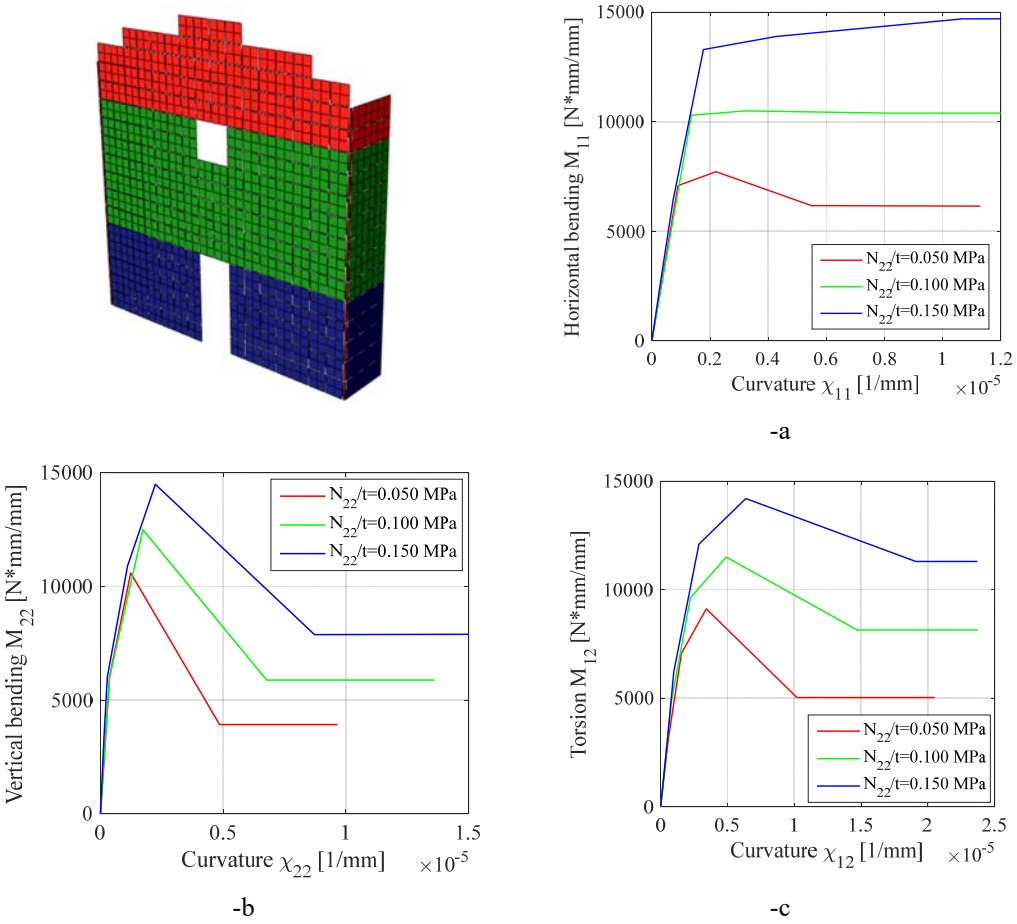

Figure 11. Moment curvature diagrams used at a structural level, Transfiguration Church. Diagrams are plotted at different levels of vertical pre-compression.

Two sets of simulations are performed in order to show the reliability of the proposed model for the seismic analyses of 3D masonry structures. First of all, the façade is analyzed using a non-linear static (pushover) approach and taking into account two distributions of forces in agreement with Italian code, one constant and the other reverse-linear along the height of the façade. Hereafter such distributions are called Mode 0 and Mode I respectively, but it is worth mentioning that in the Italian code they are labeled as G2 and G1 distributions. The results obtained using the proposed model are compared to those provided by Casolo and co-workers [22][23] in Figure 12. The control point for the displacement evaluation is placed in the upper part of the façade (tympanum center). As can be noted, there is satisfactory agreement with previously presented results, meaning that the proposed homogenization approach is able to accurately describe the elastic and inelastic behavior of real scale structures starting exclusively from the knowledge of the constituent materials mechanical properties.

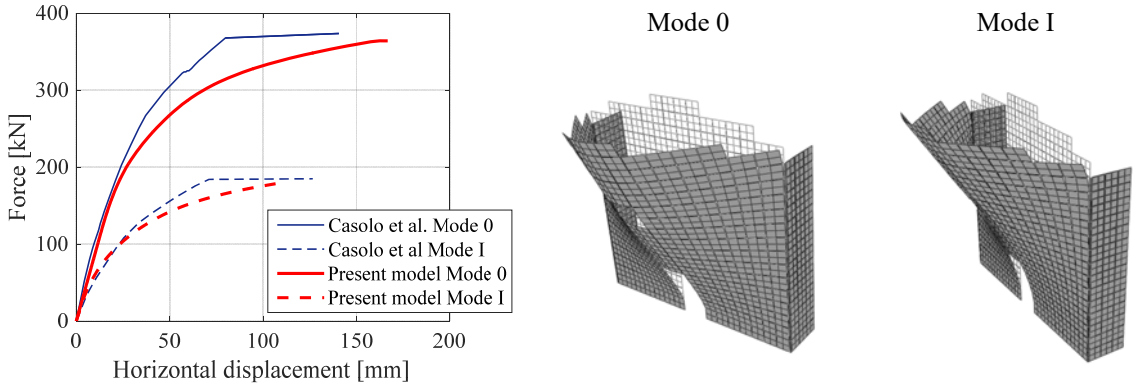

Figure 12. Pushover curves obtained (left) and corresponding deformed shapes (right)

A non-linear dynamic analysis is then performed in order to deepen the seismic behavior of the facade when subjected to natural accelerograms. The results obtained applying to the structure the Fogaria (Friuli 1976) accelerogram are summarized in Figure 13 and Figure 14.
In particular, in Figure 13 a comparison between a previous model [22][23] and present numerical results at different heights of the control point is provided, whereas Figure 14 shows the façade deformed shape and crack patterns numerically obtained at the end of the simulations(A: deformed shape. B1: vertical bending. B2: horizontal bending. B3: torsion).
As can be noted, good agreement is found between the results obtained using the proposed approach and those achieved by Casolo and co-workers [22][23], in terms of both time-displacements history and damage patterns found at the end of the simulations.
As highlighted by the residual displacement found at the end of the application of the accelerogram (Figure 13-b), the façade exhibits a collapse mechanism that mainly involves the upper part, with the resultant overturning of the tympanum. This finding suggests the activation of a slightly different failure mechanism with respect to that found in [22][23] where again the upper part is the most vulnerable, but with the formation of two inclined yield lines spreading from the upper corners down to the central rose window. Present results appear more in agreement with the expected behavior of masonry church façades. Damage patterns at the end of the simulation are depicted in Figure 14, separately for flexion and torsion as it usually occurs in RBSM models. As confirmed by the deformed shape of the façade in Figure 14-a, which clearly shows the overturning of the tympanum, high levels of damage are reached in correspondence of the horizontal line where the out-of-plane mechanism of the tympanum takes place. It is worth noting that severe damages are visible also in correspondence of the vertical edges and near the central opening, in quite reasonable agreement with the results found by Casolo and co-workers [22][23].

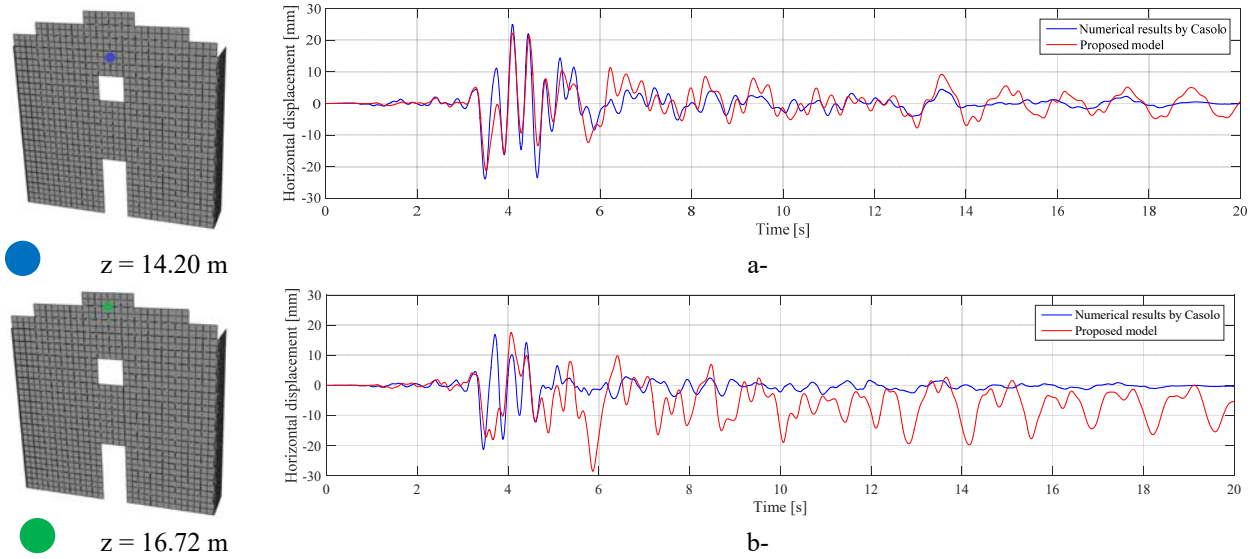

Figure 13. Comparison between previous models and present numerical results for the Transfiguration Church at different heights of the control point.

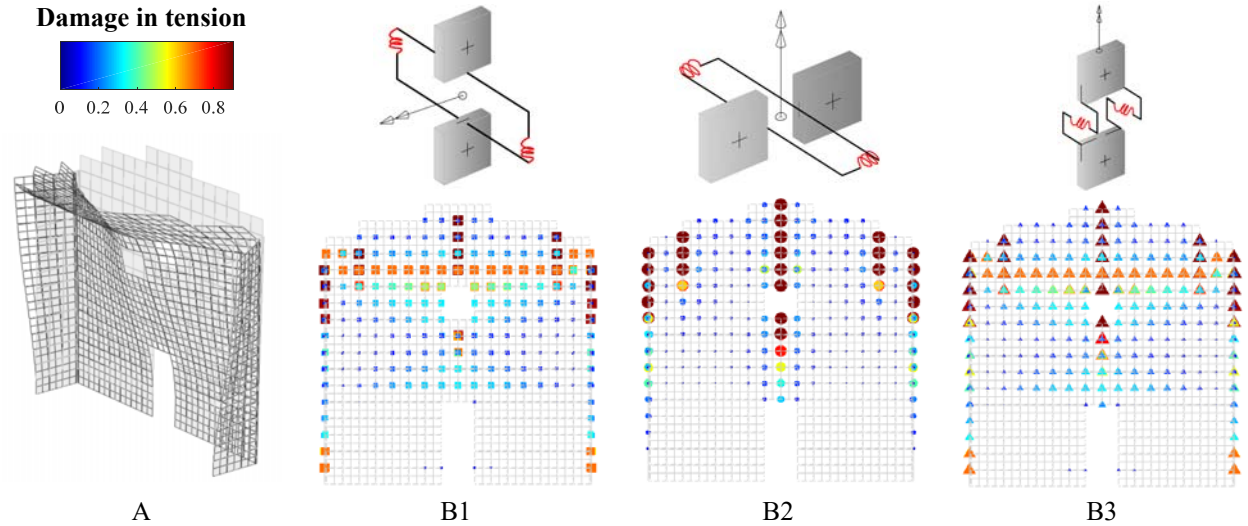

Figure 14. Deformed shape and crack patterns numerically obtained at the end of the application of the Fogaria accelerogram. A: deformed shape. B1: vertical bending. B2: horizontal bending. B3: torsion.

5 CONCLUSIONS

A simple compatible homogenization model for the non-linear static and dynamic analysis of masonry structures in- and out-of-plane loaded has been presented. The approach consists in a two-step procedure suitable for the analysis of masonry panels subjected to a variety of loads. First of all, the REV is discretized by means of triangular elastic FEs and joints are reduced to non-linear holonomic interfaces. In order to obtain quickly homogenized properties of the continuum, a pseudo analytical approach has been proposed. A series of structural analyses have been finally performed on two cases of technical relevance, namely a deep beam loaded in-plane up to collapse and a church façade subjected to equivalent static (push-over) and non-linear dynamic out-of-plane analyses. The structures have been discretized using a rigid body and spring model RBSM strategy. The springs identification has been carried

out using an energy equivalence on the stress-strain homogenized relationships deduced at the meso scale. The homogenized RBSM have been implemented into the commercial software Abaqus, where all the discussed analyses have been performed. The procedure is efficient and reliable because: (1) the homogenized mechanical properties can be directly implemented at structural level with a very limited computational effort; (2) it is not necessary to discretize with refined meshes the elementary cell; and (3) the holonomic laws assumed for mortar joints allow for a total displacement formulation of the model, where the only variables entering into the homogenization problem are represented by displacements.

REFERENCES

[1] S. Di Pasquale, New trends in the analysis of masonry structures, *Meccanica*, **27**, 173-184, 1992.

[2] P.B. Lourenço, R. de Borst, J.G. Rots, A plane stress softening plasticity model for orthotropic materials, *International Journal for Numerical Methods in Engineering*, **40**, 4033-4057, 1997.

[3] P.B. Lourenço, J. Rots, A multi-surface interface model for the analysis of masonry structures, *Journal of Engineering Mechanics ASCE*, **123** (7), 660-668, 1997.

[4] D.J. Sutcliffe, H.S. Yu, A.W. Page, Lower bound limit analysis of unreinforced masonry shear walls, *Computers & Structures*, **79**, 1295-1312, 2001.

[5] P. de Buhan, G. de Felice, A homogenization approach to the ultimate strength of brick masonry, *Journal of the Mechanics and Physics of Solids*, **45** (7), 1085-1104, 1997.

[6] P. Suquet, Analyse limite et et homogeneisation, *Comptes Rendus de l'Academie des Sciences - Series IIB – Mechanics*, **296**, 1355-1358, 1983.

[7] T. Massart, R.H.J. Peerlings, M.G.D. Geers, Mesoscopic modeling of failure and damage-induced anisotropy in brick masonry, *Eur J Mech A/Solids*, **23**, 719–35, 2004.

[8] P. Pegon, A. Anthoine, Numerical strategies for solving continuum damage problems with softening: application to the homogenization of masonry, *Computers & Structures*, **64** (1-4), 623-642, 1997.

[9] G. Milani, E. Bertolesi, Holonomic homogenized approach for the non-linear analysis of in-plane loaded masonry panels. Under review.

[10] G. Milani, P.B. Lourenço, A. Tralli, Homogenised limit analysis of masonry walls, Part I: failure surfaces, *Computers and Structures*, **84**(3-4), 166-180, 2006.

[11] G. Milani, P.B. Lourenço, A. Tralli, Homogenised limit analysis of masonry walls, Part II: structural examples, *Computers and Structures*, **84**(3-4), 181-195, 2006.

[12] G. Milani, P.B. Lourenço, A. Tralli, Homogenization approach for the limit analysis of out-of-plane loaded masonry walls, *Journal of Structural Engineering ASCE*, **132**(10), 1650-1663, 2006.

[13] G. Milani, Simple homogenization model for the non-linear analysis of in-plane loaded masonry walls, *Computers and Structures*, **89**, 1586-1601, 2011.

[14] G. Milani, Simple lower bound limit analysis homogenization model for in- and out-of-plane loaded masonry walls. *Construction & Building Materials*, **25**, 4426–4443, 2011.

[15] G. Milani, A. Tralli A, A simple meso-macro model based on SQP for the non-linear analysis of masonry double curvature structures, *International Journal of Solids and Structures*, **49**(5), 808-834, 2012.

[16] E. Bertolesi, P.B. Lourenço, G. Milani, Implementation and validation of a total displacement non-linear homogenization approach for in-plane loaded masonry. Under review.

[17] X.P. Xu, A. Needleman, Void nucleation by inclusion debonding in a crystal matrix, *Modell. Simulation Mater. Sci. Eng.*, **2**, 417-418, 1993.

[18] P. McGarry, É.Ó. Máirtín, G. Parry, G.E. Beltz, Potential-based and non-potential-based cohesive zone formulations under mixed-mode separation and over-closure. Part I: Theoretical analysis, *Journal of the Mechanics and Physics of Solids*, **63**, 336-362, 2014.

[19] E. Bertolesi, G. Milani, R. Fedele, Fast and reliable non-linear heterogeneous FE approach for the analysis of FRP-reinforced masonry arches. *Composites Part B: Engineering*, **80**, 189-200, 2016.

[20] A.W. Page, Finite element model for masonry, *J Struct Div ASCE*; **104**(8), 1267-85, 1978.

[21] P.B. Lourenço, Computational strategies for masonry structures, *PhD Thesis*, TU Delft, The Netherlands, 1996.

[22] S. Casolo, G. Uva, Nonlinear analysis of out-of-plane masonry façades: Full dynamic versus pushover methods by rigid body and spring model, *Earthquake Engineering and Structural Dynamics*, **42**(4), 499-521, 2013.

[23] S. Casolo, G. Milani, Simplified out-of-plane modeling of three-leaf masonry walls accounting for the material texture, *Construction & Building Materials*, **40**, 330–351, 2013.

[24] F. Doglioni, V. Petrini V, A. Moretti (Eds). Le chiese e il terremoto [Churches and earthquake]. LINT press, Trieste, Italy, 1994.